Carbohydrate Polymers 101 (2014) 342–348

Contents lists available at ScienceDirect

Carbohydrate Polymers

journal homepage: www.elsevier.com/locate/carbpol

Interaction with bovine serum albumin of an anti-oxidative pectic arabinogalactan from *Andrographis paniculata*

Udipta R. Chatterjee[a], Sayani Ray[a], Valérie Micard[b], Debjani Ghosh[a], Kanika Ghosh[a], Shruti S. Bandyopadhyay[a], Bimalendu Ray[a,*]

[a] Natural Products Laboratory, Department of Chemistry, The University of Burdwan, West Bengal 713104, India
[b] Montpellier SupAgro-INRA-UMII-CIRAD, UMR IATE, 2, Place Pierre Viala, 34060 Montpellier Cedex 01, France

ARTICLE INFO

Article history:
Received 4 May 2013
Received in revised form 8 September 2013
Accepted 10 September 2013
Available online 19 September 2013

Keywords:
Andrographis paniculata
Pectic arabinogalactan
Anti-oxidative effect
Protein–polysaccharide complex

ABSTRACT

A pectic arabinogalactan was obtained from the leaves of *Andrographis paniculata* by aqueous extraction followed by α-amylase treatment, deproteination, and anion exchange chromatography. Methylation analysis, Smith degradation, and NMR spectroscopy indicated that it was a highly branched arabinogalactan containing a (1 → 3)-linked β-D-Gal*p* main chain, substituted at *O*-6 by (1 → 6)-linked β-D-Gal*p* side chains. The latter residues were substituted at *O*-3 by (1 → 5)- and (1 → 3)-linked α-L-Ara*f* chains, and non reducing end-units of α-L-Ara*f* and β-D-Gal*p*. This homogeneous arabinogalactan (36 kDa), which contained phenolic acids, showed dose-dependent anti-oxidative properties. The phenolic acid moieties might be the functional sites. This arabinogalactan can form a complex with bovine serum albumin having binding constant $K = 6.48 \times 10^6$/M. Thus, this study is an important step forward to investigate the involvement of arabinogalactan in processes including interaction with biologically important transport proteins.

1. Introduction

In the mid-1950s, Denham Harman articulated a 'free-radical theory' of ageing, speculating that the endogenous oxygen radicals were generated in cells and resulted in a pattern of cumulative damage (Harman, 1956). Reactive oxygen species (ROS) are recently evidenced to be closely linked to degenerative diseases such as Alzheimer's disease, neuronal death including ischemic and hemorrhagic stroke, and acute and chronic degenerative cardiac myocyte death (Beckman & Ames, 1998; Finkel & Holbrook, 2000; Mucke, 2009). Although many drugs are proved to be successful in the management of these diseases, their use is often limited because of toxic side-effects, and the development of drug resistance. Thus, there is a need to develop new compounds with strong anti-oxidative activity accompanied by favourable pharmacological and clinical properties. Natural products have been invaluable as biologically validated platforms for drug development (Clardy & Walsh, 2004; Cragg, Grothaus, & Newman, 2009; Harvey, 2008; Newman & Cragg, 2007, 2012). In a series of review articles, Newman and colleagues (Cragg et al., 2009; Newman & Cragg, 2007, 2012) have analyzed the sources of drugs in the last 30 years. The analysis demonstrated the continuing and valuable contributions of nature as a source of lead compounds that have provided the basis and inspiration for the synthesis of new drugs (Cragg et al., 2009; Harvey, 2008; Hoye, Davoren, Wipf, Fink, & Kagan, 2008).

Andrographis paniculata, a popular ingredient of Indian herbal medicine, is widely used in the management of various diseases (Kartikar & Basu, 1975). A variety of extracts from *Andrographis* spp. and their metabolites have been examined to determine their biological activities. These included protection against allergic airway inflammation (Guan, Kong, Cheng, Lim, & Wong, 2011) and ulcerative colitis (Sandborn et al., 2013), and anti-inflammatory (Chao, Kuo, & Lin, 2010), and immunostimulatory properties (Puri et al., 1993). Till date, only secondary metabolites, namely flavonoids (Gupta, Taneja, Dhar, & Atal, 1983; Reddy et al., 2003), andrographolide (Cava, Chan, Haynes, Johnson, & Weinstein, 1962), diterpenoids (Balmain & Connolly, 1973), and noriridoids (Xu, Chou, Wang, & Wang, 2012) of this herb have been chemically characterized. Many carbohydrate polymers exhibit a large range of pharmacological effects (Baek et al., 2010; Ghosh et al., 2009, 2013; Inngjerdingen, Coulibaly, Diallo, Michaelsen, & Paulsen, 2006; Kodali, Perali, & Sen, 2011; Mantovani et al., 2008; Thakur et al., 2012), but reports on the polysaccharide component of *A. paniculata* are yet to come forth.

Biocompatibility is an important parameter in medical science as failures in compatibility may cause severe clinical complications (Kokkonen, Ilvesaro, Morra, Schols, & Tuukkanen, 2007).

* Corresponding author. Tel.: +91 342 2557709; fax: +91 342 2564452.
E-mail addresses: bimalendu_ray@yahoo.co.uk, bimalendu.ray@gmail.com (B. Ray).

0144-8617/$ – see front matter © 2013 Elsevier Ltd. All rights reserved.
http://dx.doi.org/10.1016/j.carbpol.2013.09.022

Incidentally, the distribution and metabolism of many biologically active compounds (drugs, natural products, etc) in the body are correlated with their affinities toward serum albumin (Olson & Christ, 1996). Thus the investigation of pharmacologically active molecules with respect to albumin binding is of imperative and fundamental importance.

Therefore, the aim of the present study was, first of all, to characterize the arabinogalactan from *A. paniculata.* Then the antioxidative properties of this arabinogalactan were evaluated using the free radical scavenging and ferric reducing capacity measurements. In addition, the interaction of the arabinogalactan with bovine serum albumin (BSA), the most common carrier protein, was examined.

2. Experimental

2.1. General experimental procedures

Evaporations were carried out with an Eyela N-1100 Rotary Evaporator under reduced pressure below 50 °C. Dialysis (molecular cut-off 12 kDa; Sigma–Aldrich) against distilled H_2O were performed with continuous stirring. Small volumes of sample solutions were freeze-dried with a ScanVac Cool Safe 55-F freeze drier. Moisture was determined by drying ground material in an oven at 110 °C for 3 h. Total carbohydrate content was estimated by the phenol–sulfuric acid assay (Dubois, Gilles, Hamilton, Rebers, & Smith, 1956) using glucose as standard. Total uronic acid was assayed as anhydrogalacturonic acid using *m*-hydroxydiphenyl color reagent (Ahmed & Labavitch, 1977). UV–vis spectra were recorded on a Shimadzu UV-2450 spectrophotometer, and fluorescence spectra were recorded on a Hitachi F4500 Fluorescence spectrophotometer with an excitation wave length (λ_{ex}) of 282 nm, using 10 nm excitation and 10 nm emission slit widths. GC was carried out with a Shimadzu GC-17A chromatograph fitted with a flame ionization detector, and a DB-225 column (30 m × 0.53 mm i.d.), using a program that maintained an isocratic temperature of 210 °C for 18 min and helium as gas vector. GC–MS was performed with a Shimadzu QP 5050A GC–MS instrument at 70 eV. Conditions for GC–MS were as described previously (Mazumder, Morvan, Thakur, & Ray, 2004). ^{1}H NMR spectrum was recorded on a Bruker DRX-500 NMR spectrometer at 25 °C in D_2O solvent. The ^{13}C NMR spectrum of F3 was recorded on a Bruker AVANCE III 400 MHz spectrometer using 1.36 s acquisition time, 24038 Hz spectral width, and 1 s relaxation delay. Gel permeation chromatography was performed on a Sephacryl™ S-100 HR column (Amersham Biosciences AB, 2.6 cm × 90 cm; V_0 145 mL, V_t 378 mL) using 0.5 M NaOAc buffer (pH 5.0) as eluent at 0.5 mL/min. Solutions (12 mL) containing 10 mg/mL of the polysaccharide were injected, and the eluate was monitored by the PhOH–H_2SO_4 reaction (Dubois et al., 1956).

2.2. Plant material and preliminary treatments

Powdered leaves (Batch No: 006006TK, Product Code: 0066TK38) of *A. paniculata* (Non Timber Forest Produce Division, TAIPU NTFP BEAT, Darjeeling, Govt. of West Bengal, India) was extracted successively with n-hexane, EtOH, and $CHCl_3$–CH_3OH (1:1, v/v) for 18 h (each) in a Soxhlet extractor.

2.3. Extraction and purification of the arabinogalactan

Polysaccharides were extracted from the defatted powder (200 g) by stirring with 4 L of H_2O (pH 6.0) at 4–8 °C for 12 h. After filtration, the insoluble material was treated with 4 L of H_2O (×3), sequentially, at 25–30 °C for 12 h each. The combined extracts were concentrated, and a polymeric fraction was isolated by precipitation with EtOH (8 L) and centrifugation. The precipitates were dissolved in H_2O and the resulting solution was treated with α-amylase (Sisco Research Laboratories Pvt. Ltd.) 100 units/mL of the enzyme in 60 mM phosphate buffer (pH 7.0), containing 7 mM NaCl, at 20–27 °C for 24 h. The resulting solution was dialysed, cooled (<4 °C) and then treated with cold 10% aqueous CCl_3CO_2H on ice (<4 °C) for protein removal. After 1 h, the reaction mixture was centrifuged and the pH of supernatant was adjusted to 6.0 by slow addition of 0.5 N NaOH (<4 °C). The resulting solution dialyzed, and then lyophilized to yield the water extracted carbohydrate polymer (CP, 11 g). A solution (100 mL) of CP in 0.05 M NaOAc (pH 5.5) was applied to a column (2.6 cm × 80 cm) of DEAE Sepharose Fast Flow (AcO^-; Amersham Biosciences AB). Thereafter, the column was eluted (2 mL/min) successively with 0.05 M (fraction F1), 0.2 M (fraction F2), and 1 M (fraction F3) NaOAc buffer (pH 5.5) in a stepwise manner.

2.4. Molecular mass

The molecular mass was determined by high-performance size-exclusion chromatography (Shimadzu), with two columns (HEMA-BIO 300 followed by HEMA-BIO 100) in series (each column 8 mm × 250 mm), using a refractive index detector and the eluent was 0.1 M $NaNO_3$. A set of pullulan standards was used for calibration of the column (Gearing Scientific Ltd.).

2.5. Monosaccharide analysis

Neutral sugars were analysed after hydrolysis with 1 M H_2SO_4 (3 h, 100 °C). The released monosaccharide residues were reduced ($NaBH_4$), acetylated (Ac_2O) and analyzed as their alditol acetate (Blakeney, Harris, Henry, & Bruce, 1983) by GC–MS. Monosaccharides in the acid hydrolysate were also analyzed by thin layer chromatography on kieselgel 60F plate (Merck) using EtOH/PhOH/Pyridine/0.1 M H_3PO_4 (5/1/1/2, v/v) as eluent. Monosaccharides were then detected by heating at 100 °C after treatment with saturated solution of aniline phthalate. The monosaccharide composition was also determined after methanolysis (MeOH/HCl 2.0 N, 18 h, 80 °C) by GC analysis of the *per-O*-trimethyl-silylated methyl glycosides (York, Darvill, O'Neil, Stevenson, & Albersheim, 1985).

2.6. Phenolics analysis

Total polyphenolic content was estimated according to the Folin-Ciocalteu method using gallic acid as standard and the result was expressed as milligrams of gallic acid equivalent per gram of sample. The polymer which was supposed to be ester-linked phenolic acid was saponified by dissolving 50 mg F3 in 1 mL 0.1 N NaOH under N_2 at 35 °C. An internal standard (2,3,5-trimethoxy-(*E*)-cinnamic acid (TMCA), T-4002, Sigma Chemical Co.) was added before adjusting pH to 2 with 2 N HCl. Phenolic acids were then extracted with Et_2O and quantified by RP-HPLC as described (Antoine et al., 2003). The response factors of the *p*-coumaric acid (*p*-CA) and the 4-*O*-8′, 5′-5′′-dehydrotriferulic acid (ferulic acid trimer, tri-FA) relative to the internal standard were determined at 320 nm with pure compounds. All analyses were performed at least in duplicate, with c.v. < 10% (mean c.v. 1/4 3% for *p*-CA and 8% for tri-FA). The water soluble material was then dialysed and lyophilized to yield the degraded product named as F3D.

2.7. Smith degradation

Periodate oxidation was carried out according to Goldstein, Hay, Lewis, and Smith (1965) with modification. Briefly, a solution of 600 mg arabinogalactan (F3) in 200 mL of reagent (50 mM $NaIO_4$ made up in 0.25 M HCO_2H, pH adjusted to 3.7 with 0.5 M NaOH) was

incubated at 4–8 °C in the dark for 6 days with occasional stirring. The reaction was terminated by adding 1,2-ethanediol (4 mL). After reduction with an excess of $NaBH_4$ (1.5 g) and desalting by dialysis (1 kDa cutoff membranes), the product was partially hydrolyzed with CF_3CO_2H, pH 2.0, for 30 min at 100 °C, and neutralized. The Smith degraded product (SD, 150 mg) was isolated by lyophilization of the dialyzed product. A part (110 mg) of SD was subjected to a second Smith degradation using similar protocol and the resultant periodate resistant carbohydrate polymer has been designated as SD2 (39 mg).

2.8. Glycosidic linkage analysis

Methylation was carried out by the method of Sims and Bacic (1995). Prior to methylation, the uronic acids present in carbohydrate polymer were reduced to primary alcohols on the polymer level (F3R) using the method of Kim and Carpita (1992) except that $NaBH_4$ was used instead of $NaBD_4$. In the methylation procedure, free hydroxyl groups in the carbohydrates were de-protonated and methylated (CH_3I), then the glycosidic linkages were hydrolyzed (2 M CF_3CO_2H, 3 h, 100 °C), and the partially methylated monosaccharides were reduced ($NaBD_4$) and acetylated (Ac_2O), and analyzed by GC and GC–MS as described (Blakeney & Stone, 1985). The partially methylated alditol acetates (PMAAs) were identified by the measurement of relative retention times, methoxyl substitution pattern as obtained from GC–MS and carbohydrate composition of the non-methylated polymers. Molar ratios of PMAAs were calculated from peak areas using response factors as described (Sweet, Shapiro, & Albersheim, 1975).

2.9. 1,1-Diphenyl-2-picrylhydrazyl (DPPH) radical assay

The free radical scavenging capacity of samples was determined by a modified DPPH radical assay (Huang, Ou, & Prior, 2005) using butylated hydroxy anisole (BHA) and butylated hydroxy toluene (BHT) as standard. For this assay, 1 mL of freshly prepared methanolic DPPH radical (0.008%) solution was added to 1 mL of sample or standard (solvent for the blank). The mixture was incubated at 30 °C for 1 h, and the absorbance was measured at 515 nm against blank. The absorbance of DPPH radical was measured at this wavelength against methanol blank. The DPPH radical scavenging capacity was calculated using the equation:

$$\text{inhibition}\,(\%) = \left[\frac{A_1 - A_2}{A_1}\right] \times 100$$

where A_1 is the absorbance of DPPH radical solution and A_2 is the absorbance of the sample or standard.

2.10. Ferric reducing anti-oxidant potential (FRAP) assay

The FRAP assays were conducted according to Benzie and Strain (1996). Standard curves were prepared using various concentrations (100–2000 mg/L) of $FeSO_4, 7H_2O$ for 4 min and 30 min. Similar curves for samples were also drawn. Results are expressed as the Equivalent Concentration 1 (EC_1, i.e., the concentration of antioxidant having a ferric-TPTZ reducing ability equivalent to that of 1 mM $FeSO_4{\cdot}7H_2O$). EC_1 values were calculated as the concentration of samples giving an absorbance increase in the FRAP assay equivalent to the theoretical absorbance value of 1 mM concentration of Fe(II) solution determined using the corresponding regression equation.

2.11. BSA–arabinogalactan interaction

Ultraviolet–visible (UV–vis) spectra. UV–vis absorption spectra of 3.6 μM BSA in absence and presence of 0.347–2.083 μM arabinogalactan in a 100 mM phosphate buffer (pH 7.4) were recorded at 25 °C. The spectra of 0.347–2.083 μM arabinogalactan were also recorded under similar condition as blank in order to measure the spectral inferences on the BSA–polysaccharide system.

Fluorescence quenching measurements. The linear range of bovine serum albumin (BSA) fluorescence in 100 mM phosphate buffer at pH 7.4 is between 0 and 2.25 μM. Therefore, 0.75 μM BSA was chosen as the concentration for fluorescence experiments. A dilution series of arabinogalactan with increasing concentrations (0.086–2.778 μM) were prepared in the same buffer. For each data point, 1 mL of the appropriate arabinogalactan solution was added into 1 mL BSA (1.5 μM) solution, to give a final concentration of arabinogalactan in the range (0.043–1.389 μM). The change in fluorescence emission spectra were measured within 1 min of adding arabinogalactan to the BSA. To eliminate the background effect on BSA, the fluorescence spectra of this polymer solution of each concentration were measured at 282 nm as a blank titration series (i.e., adding 1 mL of each carbohydrate polymer concentration into 1 mL buffer). The fluorescence intensity values obtained at λ_{em} of BSA were then subtracted from the fluorescence intensity values obtained for BSA quenching. The results from fluorescence measurements were used to determine the binding constant of carbohydrate polymer–protein interaction using the modified Stern–Volmer equation:

$$\frac{F_0}{(F_0 - F)} = \frac{1}{f\,K[Q]} + \frac{1}{f}$$

where F and F_0 are current and initial fluorescence intensities, respectively. K is the Stern–Volmer quenching constant, $[Q]$ is quencher concentration, and f is the fraction of the initial fluorescence that is accessible to quencher. In the present study, carbohydrate polymer is considered as quencher. The plot of $F_0/(F_0 - F)$ vs. $1/[Q]$ yields $1/f$ as the intercept and $1/(f{\cdot}K)$ as the slope. Thus, the ratio of intercept and slope gives K.

3. Results and discussion

3.1. Extraction, purification and chemical composition of the carbohydrate polymer

Defatted leaves of *A. paniculata* were extracted with H_2O, and the extract was treated with EtOH, to obtain a crude precipitate of polymers (Scheme 1). It was then treated, sequentially, with α-amylase and trichloro acetic acid to yield the crude carbohydrate polymer (CP). This material was further fractionated by anion exchange chromatography, giving three fractions F1 (13%), F2 (15%) and F3 (72%), which were eluted with 0.05, 0.2 and 1.0 M NaOAc, respectively. The recovery yield from the anion exchanger was 91% on total sugar basis. Size exclusion chromatographic analysis of the major fraction (F3) showed the presence of a homogeneous polymer with a molecular mass of 36 kDa. This fraction was found to be an arabinogalactan containing galatose, arabinose, galacturonic acid, glucose, and rhamnose in the molar ratio of 59:28:11:1:1. This arabinogalactan possessed phenolic acids (80 mg of gallic acid equivalent per gram of sample) including ferulic acid, coumaric acid, sinapic acid and the following diferulic acid (diFA) forms 8,6′-diFA, and 8,6′-benzofuran-diFA in a molar ratio of 56:20:10:8:6. The majority of ferulic acid was present in the (*E*)-form. The carboxyl reduced derivative of F3 (F3R) contained galactose, arabinose, glucose, and rhamnose in a 67:29:1:3 molar ratio.

3.2. Glycosidic linkage analysis suggested the presence of highly branched pectic arabinogalactan

The results obtained from the glycosidic linkage analysis of F3, as summarized in Table 1, revealed the presence of a highly branched

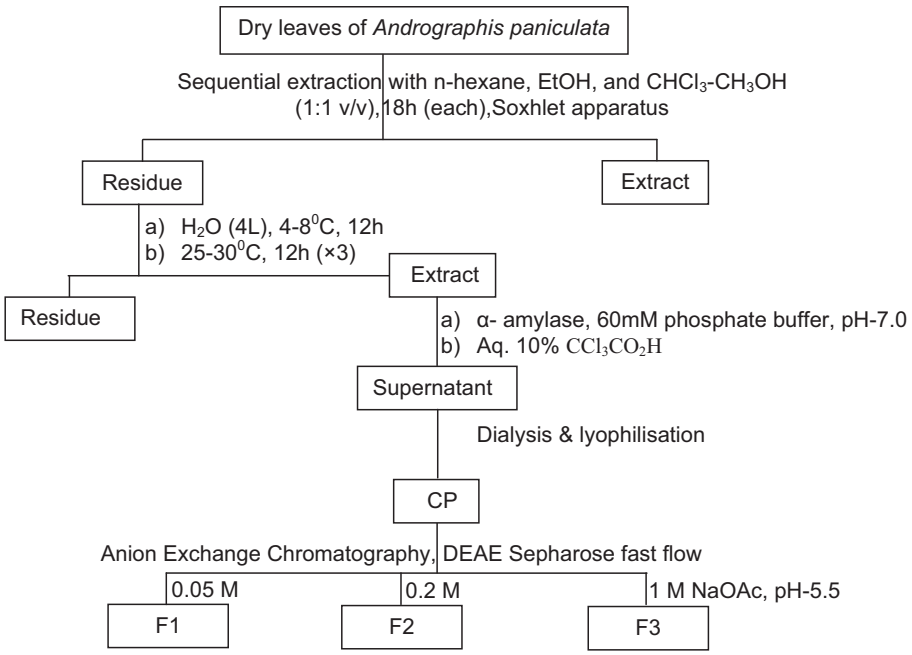

Scheme 1. Extraction and purification of a pectic arabinogalactan from *A. paniculata* leaves.

Table 1
Partially *O*-methylalditol acetates formed on methylation analysis of the arabinogalactan (F3) of *Andrographis paniculata* and its carboxyl reduced (F3R) and Smith degraded (SD and SD2) derivatives.

Methylation products[a]	Linkages	Molar ratios			
		F3	F3R	SD	SD2
2,3,5-Me_3-Ara	Terminal-	25	22	18	0
2,5-Me_2-Ara	1,3-	10	8	0	0
2,3-Me_2-Ara	1,4- &/or 1,5-	2	2	0	0
2,3,6-Me_3-Glc	1,4-	1	1	0	0
3,4-Me_2-Rha	1,2-	0	1	0	0
3-Me-Rha	1,2,4-	0	2	0	0
2,3,4,6-Me_4-Gal	Terminal-	9	8	11	19
2,4,6-Me_3-Gal	1,3-	10	9	24	49
2,3,6-Me_3-Gal	1,4-	1	10	0	0
2,3,4-Me_3-Gal	1,6-	16	14	20	17
2,4-Me_2-Gal	1,3,6-	27	24	26	15

[a] 2,3,5-Me_3-Ara denotes 1,4-di-*O*-acetyl-2,3,5-tri-*O*-methylarabinitol, etc.

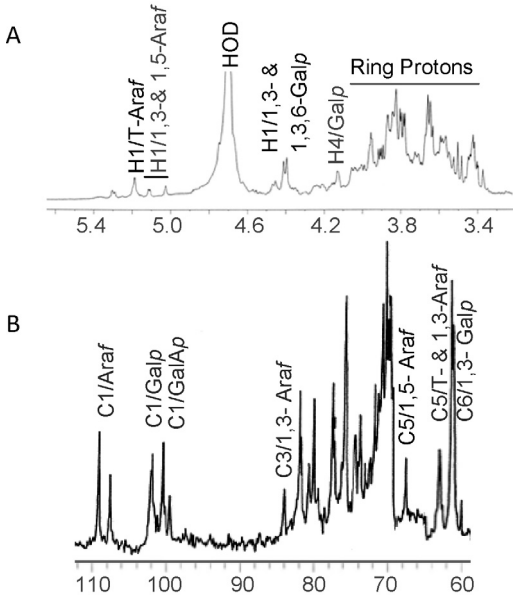

Fig. 1. (A) ^{1}H and (B) ^{13}C NMR spectra of the arabinogalactan (F3) of *A. paniculata*. The spectra of the macromolecule were recorded at 25 °C in D_2O solution. Numerical values are in δ (ppm). The signal for deuterated water is designated as HOD.

arabinogalactan, containing nonreducing end-units of Ara*f* (2,3,5-Me_3-Ara) and Gal*p* (2,3,4,6-Me_4-Gal). The galactopyranosyl units were, mainly, 3-*O*-, 6-*O*- and 3,6-di-*O*-substituted, in accord with 2,4,6-Me_3-Gal, 2,3,4-Me_3-Gal and 2,4-Me_2-Gal methylated derivatives, respectively. The arabinosyl units were substituted at *O*-3, and *O*-5 (Ara*f*) and/or *O*-4 (Ara*p*), in accord with 2,5-Me_2-Ara, and 2,3-Me_2-Ara derivatives, respectively. The arabinosyl units in arabinogalactan were in the Ara*f* form in accord with the presence of ^{13}C NMR signals in the range of 109.0–107.5 ppm (Fig. 1). The increase in the percentage of the 2,3,6-Me_3-Gal derivative observed after carboxy-reduction (F3R) could be due to the presence of a pectic chain formed by Gal*p*A (1 → 4)-linked to Rha*p* at *O*-2. The rhamnosyl units were 2-*O*- and 2,4-di-*O*-substituted, as demonstrated by the presence of 3,4-Me_2-Rha and 3-Me-Rha derivatives, respectively. Therefore, this arabinogalactan is linked to 4-*O*- of some Rha*p* units of a type I rhamnogalacturonan, formed by repeating (1 → 4)-α-Gal*p*A-(1 → 2)-α-Rha*p* units.

The anomeric signals in the ^{1}H NMR spectrum (Fig. 1) of arabinogalactan F3 were assigned according to sugar composition and glycosidic linkage makeup, and data in the literature (Cipriani et al., 2006; Ozaki, Oki, Suzuki, & Kitamura, 2010; Sims & Furneaux, 2003; Xu, Dong, Qiu, Cong, & Ding, 2010). The signal at δ 5.19 was assigned to anomeric protons (H1) of the nonreducing terminal α-Ara$_f$, and the signals at δ 5.04 and δ 5.13 originated from the anomeric protons (H1) of 1,5- and 1,3-linked α-Ara*f*, respectively. The signals of Gal and those of Ara could be easily differentiated since F3 is made up mainly of Gal and Ara residues. This arabinogalactan also showed one group of H1 signals from δ 4.39 to 4.41 and a second group of H1 signals from δ 4.45 to 4.47 originating from resonances of anomeric protons (H1) of different β-Gal*p* residues of the β-1,3-linked galactan backbone (Ozaki et al., 2010). The signal at δ 4.13was assigned to H4 protons of β-Gal*p* residues. This spectrum also contain resonances characteristic of ring protons (H2–H5) between 3.37 and 4.08 ppm.

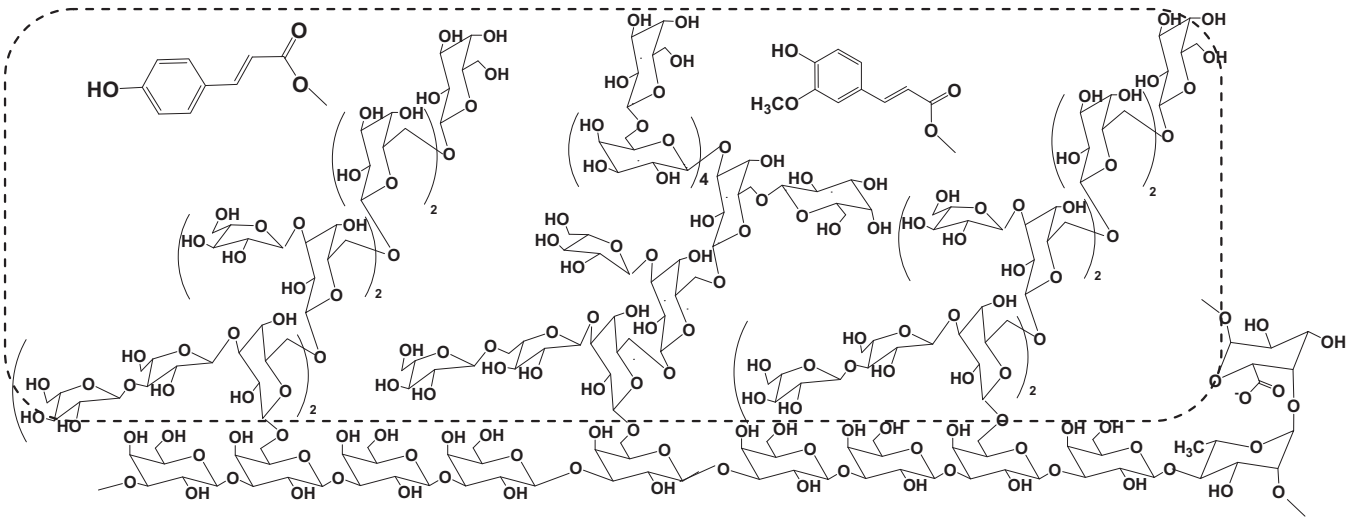

Fig. 2. A theoretical structural model for the arabinogalactan (F3) of *A. paniculata*.

As shown in Fig. 1B the ^{13}C NMR spectrum of F3 contained signals harmonious with an arabinogalactan, with signals at δ 109.0 and δ 107.5 of C1 of arabinofuranosyl residues. The chemical shifts indicated α-anomeric configuration. The strong overlapping signals around 101.9 could be attributed to variously linked β-Gal*p* residues. The signal around δ 99.7 was assigned to α-GalA, in reference to value found in the literature (Nie et al., 2013). The signal for C6 of Rha residues was not detected, but it is hardly surprising given its low abundance. Surprisingly, signals characteristics of phenolic moieties, like the arabinogalactan of *Enhydra fluctuans* that contained esterified phenolic acids, were not observed (Ghosh et al., 2013). Signals around δ 83.9 was assigned to C3 of (1 → 3)-linked Ara*f*. It also showed one group of signals from δ 59.8 to 62.2 of C5 of terminal- and (1 → 3)-linked Ara*f*, and C6 of (1 → 3)-Gal*p* residues in reference to values found in the literature (Cipriani et al., 2006; Ghosh et al., 2013; Ozaki et al., 2010; Sims & Furneaux, 2003; Xu et al., 2010).

3.3. Smith degradation study revealed the presence of large side chains containing Gal and Ara residues

Periodate oxidation of this arabinogalactan was carried out to characterize its molecular structure. The Smith degraded polymer (SD) contained galactose and arabinose in a molar ratio of 87:13. The galacturonic acids and the majority of arabinosyl units were eliminated on periodate oxidation. Glycosidic linkage analysis (Table 1) showed that arabinosyl units present in SD were all non reducing terminal units, characterized by the presence of 2,3,5-Me_3-Ara only. Non reducing terminal units of Gal*p* were also present, according to the appearance of the 2,3,4,6-Me_4-Gal derivative. The other derivatives found in SD were 2,4,6-Me_3-Gal, 2,3,4-Me_3-Gal, and 2,4-Me_2-Gal. The SD fraction upon submission to a second Smith degradation gave rise another periodate-resistant polysaccharide (SD2) containing solely of galactosyl units, indicating that arabinose residues were components of side chains. The results of Smith degradation study showed that the molecular core of the pectic arabinogalactan (F3) of present study was constituted by 3-*O*-, and 3,6-di-*O*-substituted galactopyranosyl units, substituted at *O*-6 by (1 → 6)-linked β-Gal*p* side chains. The latter were mainly substituted at *O*-3 by (1 → 5)-, and (1 → 3)-linked α-Ara*f* chains, and nonreducing end-units of α-Ara*f* and β-D-Gal*p*. On the basis of the data obtained, it was concluded that the arabinogalactan of *A. paniculata* has the theoretical structure shown in Fig. 2.

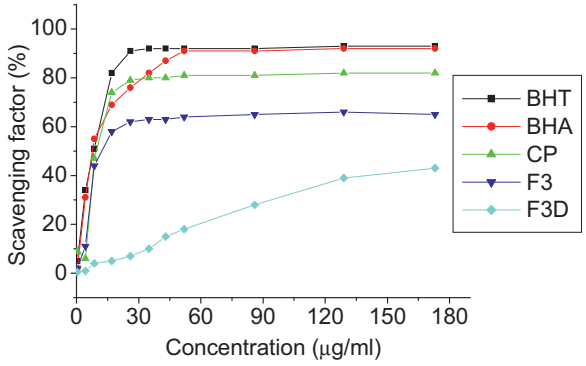

Fig. 3. Scavenging effect on DPPH radicals of carbohydrate polymer (CP), the purified arabinogalactan (F3) and the de-esterified arabinogalactan (F3D) of *A. paniculata* along with standard anti-oxidants BHA (Butylated hydroxy anisole) and BHT (butylated hydroxy toluene).

3.4. Anti-oxidative properties of the arabinogalactan

As shown in Fig. 3, the crude and purified arabinogalactan (CP and F3) exhibited dose dependent DPPH-radical scavenging activity in the concentration range 4–52 μg/mL. At the concentration of 52 μg/mL the fraction CP scavenged 81% DPPH radicals, whereas BHT and BHA exhibited 89 and 88% activity, respectively. The scavenging value of F3 is 64% whereas that of F3D is 18% at this concentration indicating that its anti-oxidative capacity decreased after removal of the esterified phenolic acids. Notably, the crude CP has higher activity than F3. However, the crude fraction (CP) is made of three fractions. These fractions can have their own activities, which may act synergistically to make the whole CP activity higher than that of the purified fraction (F3). The variation in activity between crude and purified product has also been observed by other investigators (Inngjerdingen et al., 2006). Even the potency of different regions of a pectic polymer may also vary significantly (Kiyohara, Cyong, & Yamada, 1988). This arabinogalactan also showed protective effect on FRAP assay. The EC_1 values of CP were 862 μg/mL and 542 μg/mL, and that of F3 were 876 μg/mL and 622 μg/mL at 4 and 30 min of reaction, respectively indicating that its anti-oxidative capacity increased with time.

Regarding structure–function relationship, the arabinogalactan of present study contains ester linked phenolic acids, which can prevent oxidative stress by direct scavenging of free radicals. In this way, phenolic acid becomes oxidized and forms a more

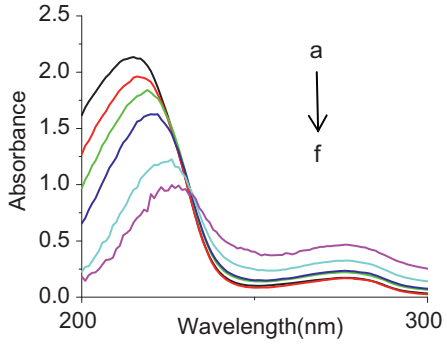

Fig. 4. Effect of arabinogalactan (F3) of *A. paniculata* on the UV absorption of BSA in 100 mM phosphate buffer at pH 7.4. The black line is the spectrum of native 3.6 μM BSA (a). The colored lines correspond to the spectra of BSA induced by various arabinogalactan (F3) concentration: b → f (0.347, 0.694, 1.042, 1.736 and 2.083 μM).

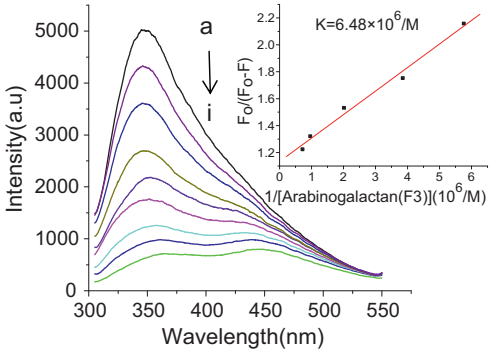

Fig. 5. Fluorescence emission spectra of bovine serum albumin in absence and presence of various concentration of arabinogalactan (F3) of *A. paniculata* at excitation wavelengths 282 nm in 100 mM phosphate buffer at pH 7.4. (a) 0.75 μM free BSA; (b → i) 0.75 μM BSA with 0.043, 0.087, 0.129, 0.174, 0.259, 0.496, 1.042 and 1.389 μM arabinogalactan (F3). Inset: The plot of $F_0/(F_0 - F)$ versus 1/[arabinogalactan(F3)](10^6/M) with the binding constant K (the ratio of the intercept to slope) for arabinogalactan–BSA complex.

stable and less reactive radical. Notably, the activity of de-esterified material F3D is lower than that of CP or F3. Consequently, the phenolic acid moieties seem to be the active functional sites of this arabinogalactan.

3.5. Formation of BSA–arabinogalactan complex is driven by electrostatic interaction

The UV–vis spectra (Fig. 4) of BSA at pH 7.4 in the absence and presence of arabinogalactan (F3) contained two absorption peaks at 219 and 278 nm, attributed to the π–π* transition of characteristic polypeptide backbone structure and *n*–π* transition of aromatic amino acids, respectively (Zhao, Liu, Chi, Teng, & Qin, 2010). With gradual addition of the arabinogalactan to BSA solution, the intensity of the peak at 219 nm decreases and the λ_{max} for the particles in the solution shifted towards longer wavelength (9 nm). These spectral changes might arise from the disturbance of the microenvironment around the polypeptide caused by the binding of arabinogalactan with BSA. Such complex formation that occurs above the isoelectric point (*p*I) of BSA (*p*I = 4.7) may be attributed to the electrostatic interaction between positively charged patches (Park, Muhoberac, Dubin, & Xia, 1992; Shu, Liu, Chen, Chen, & Wang, 2011) of the BSA and negatively charged pectic arabinogalactan. Remarkably, the intensity of the peak at 278 nm related to the *n*–π* transition of aromatic amino acids also changes at this pH suggesting that the microenvironment of the aromatic amino acid is changed. Moreover, arabinogalactan binds with BSA in a dose dependent manner (Fig. 4) and the formed complex was water soluble.

The formation of complex between arabinogalactan and BSA was further confirmed by fluorescence quenching measurement. As shown in Fig. 5 the intrinsic fluorescence emission spectra for BSA in the presence of increasing concentrations of fraction F3 (0.043–1.389 μM) showed a concentration dependent decrease in intensity with a red shift (12.2 nm in presence of 0.496 μM F3). The arabinogalactan absorbed a small portion of the 282 nm excitation light used and fluoresced around 372 nm. However, the contribution of arabinogalactan to overall fluorescence for most of concentrations remained negligible. Consequently, the observed red shift was due to the complexation of arabinogalactan with BSA. There are two tryptophans (Trp) in BSA at positions 134 and 212 located in sub domains IB and IIA (Peters, 1985). Trp-134 is thought to be more solvent-exposed than Trp-212 as the former is located on the surface of the BSA molecule. Thus, it is likely that this quenching is due to Trp-134 residues, which are more accessible to quencher arabinogalactan ($M_{av} \sim 36$ kDa) compared to Trp-212. The quenching constant can be taken as the binding constant of the complexation reaction between fluorophore and quencher. The binding constant for arabinogalactan–BSA complexation is $K = 6.48 \times 10^6$/M. Thus, the formation of water-soluble complex driven by the electrostatic interaction of the positively charged patches of the BSA and arabinogalactan was established. This observation is important as the distribution and metabolism of many biologically active compounds in the body are correlated with their affinities toward serum albumin.

4. Conclusions

In conclusion, the findings of this study highlight several novel and important aspects of the *A. paniculata* derived pectic arabinogalactan with regard to its structures and biological effects: (i) a 36 kDa arabinogalactan containing esterified phenolic acids in monomeric and dimeric forms could be extracted using traditional water extraction method, (ii) the anti-oxidative properties of this polymer are comparable with standard anti-oxidants, (iii) the phenolic acid moieties are the important functional sites, (iv) this polymer can form water-soluble complex with bovine serum albumin and changes its microenvironment, (v) at pH = 7.4, the driving force behind complex formation is the electrostatic interaction between the positively charged patches of BSA and anionic arabinogalactan, and (vi) fluorescence and UV–vis spectroscopy are important techniques to study the interaction between BSA and pectic arabinogalactan containing esterified phenolic acids. Finally, the biological activity of the arabinogalactan of *A. paniculata* provides a scientific basis for the use of this herb in traditional medicine.

Acknowledgements

Financial support from Department of Science and Technology (SR/S1/OC-38/2012), New Delhi, India to B. Ray is gratefully acknowledged. Authors are very thankful to Aurélie Putois (INRA, Montpellier, France) for her technical assistance for the determination of the phenolic acids.

References

Ahmed, A., & Labavitch, J. M. (1977). A simplified method for accurate determination of cell wall uronide content. *Journal of Food Biochemistry, 1*, 361–365.

Antoine, C., Peyron, S., Mabille, F., Lapierre, C., Bouchet, B., Abecassis, J., et al. (2003). Individual contribution of grain outer layers and their cell wall structure to the mechanical properties of *Wheat bran*. *Journal of Agricultural and Food Chemistry, 51*, 2026–2033.

Baek, S. H., Lee, J. G., Park, S. Y., Bae, O. N., Kim, D. H., & Park, J. H. (2010). Pectic polysaccharides from *Panax ginseng* as the antirotavirus principals in ginseng. *Biomacromolecules*, *11*, 2044–2052.

Balmain, A., & Connolly, J. D. (1973). Minor diterpenoid constituents of *Andrographis paniculata* Nees. *Journal of the Chemical Society Perkin Transactions 1*, *12*, 1247–1251.

Beckman, K. B., & Ames, B. N. (1998). The free radical theory of aging matures. *Physiological Review*, *78*, 547–581.

Benzie, I. F. F., & Strain, J. J. (1996). The ferric reducing ability of plasma (FRAP) as a measure of antioxidant power: The FRAP assay. *Analytical Biochemistry*, *239*, 70–76.

Blakeney, A. B., Harris, P., Henry, R. J., & Bruce, A. B. (1983). A simple rapid preparation of alditol acetates for monosaccharide analysis. *Carbohydrate Research*, *113*, 291–299.

Blakeney, A. B., & Stone, B. A. (1985). Methylation of carbohydrates with lithium methylsulphinyl carbanion. *Carbohydrate Research*, *140*, 319–324.

Cava, M. P., Chan, W. R., Haynes, L. J., Johnson, L. F., & Weinstein, B. (1962). The structure of andrographolide. *Tetrahedron*, *18*, 397–403.

Chao, W.-W., Kuo, Y.-H., & Lin, B.-F. (2010). Anti-inflammatory activity of new compounds from *Andrographis paniculata* by NF-κB trans activation inhibition. *Journal of Agricultural and Food Chemistry*, *58*, 2505–2512.

Cipriani, T. R., Mellinger, C. G., de Souza, L. M., Baggio, C. H., Freitas, C. S., Marques, M. C. A., et al. (2006). A polysaccharide from a tea (Infusion) of *Maytenus ilicifolia* leaves with anti-ulcer protective effects. *Journal of Natural Products*, *69*, 1018–1021.

Clardy, J., & Walsh, C. (2004). Lessons from natural molecules. *Nature*, *432*, 829–837.

Cragg, G. M., Grothaus, P. G., & Newman, D. J. (2009). Impact of natural products on developing new anti-cancer agents. *Chemical Review*, *109*, 3012–3043.

Dubois, M., Gilles, K. A., Hamilton, J. K., Rebers, P. A., & Smith, F. (1956). Colorimetric method for determination of sugars and related substances. *Analytical Chemistry*, *28*, 350–366.

Finkel, T., & Holbrook, N. J. (2000). Oxidants, oxidative stress and the biology of aging. *Nature*, *408*, 239–247.

Ghosh, D., Ray, S., Ghosh, K., Micard, V., Chatterjee, U. R., Ghosal, P. K., et al. (2013). Antioxidative carbohydrate polymer from *Enhydra fluctuans* and its interaction with bovine serum albumin. *Biomacromolecules*, *14*, 1761–1768.

Ghosh, T., Chattopadhyay, K., Marschall, M., Karmakar, P., Mandal, P., & Ray, B. (2009). Focus on anti-virally active sulfated polysaccharides: From structure–activity analysis to clinical evaluation. *Glycobiology*, *19*, 2–15.

Goldstein, I. J., Hay, G. W., Lewis, B. A., & Smith, F. (1965). Controlled degradation of polysaccharides by periodate oxidation, reduction, and hydrolysis. In R. L. Whistler, & J. N. BeMiller (Eds.), *Methods in carbohydrate chemistry* (Vol. 5) (pp. 361–370). New York: Academic Press.

Guan, S.-P., Kong, L.-R., Cheng, C., Lim, J. C. W., & Wong, W. S. F. (2011). Protective role of 14-deoxy-11,12-didehydroandrographolide, a noncytotoxic analogue of andrographolide, in allergic airway inflammation. *Journal of Natural Products*, *74*, 1484–1490.

Gupta, K. K., Taneja, S. C., Dhar, K. L., & Atal, C. K. (1983). Flavonoids of *Andrographis paniculata*. *Phytochemistry*, *22*, 314–315.

Harman, D. (1956). Aging: A theory based on free radical and radiation chemistry. *Journal of Gerontology*, *11*, 298–300.

Harvey, A. L. (2008). Natural products in drug discovery. *Drug Discovery Today*, *13*, 894–941.

Hoye, A. T., Davoren, J. E., Wipf, P., Fink, M. P., & Kagan, V. E. (2008). Targeting mitochondria. *Accounts of Chemical Research*, *41*, 87–97.

Huang, D., Ou, B., & Prior, R. L. (2005). The chemistry behind antioxidant capacity assays. *Journal of Agriculture and Food Chemistry*, *53*, 1841–1856.

Inngjerdingen, K. T., Coulibaly, A., Diallo, D., Michaelsen, T. E., & Paulsen, B. S. (2006). A complement fixing polysaccharide from *Biophytum petersianum* Klotzsch, a medicinal plant from Mali, West Africa. *Biomacromolecules*, *7*, 48–53.

Kartikar, K. R., & Basu, B. D. (1975). . *Indian medicinal plants* (vol. 3) New Delhi, India: Periodical Experts.

Kim, J. B., & Carpita, N. C. (1992). Changes in esterification of the uronic acid groups of cell wall polysaccharides during elongation of *Maize coleoptiles*. *Plant Physiology*, *98*, 646–653.

Kiyohara, H., Cyong, J. C., & Yamada, H. (1988). Structure and anticomplementary activity of pectic polysaccharides isolated from the root of *Angelica acutiloba* Kitagawa. *Carbohydrate Research*, *182*, 259–275.

Kodali, V. P., Perali, R. S., & Sen, R. (2011). Purification and partial elucidation of the structure of an antioxidant carbohydrate biopolymer from the probiotic bacterium *Bacillus coagulans* RK-02. *Journal of Natural Products*, *74*, 1692–1697.

Kokkonen, H. E., Ilvesaro, J. M., Morra, M., Schols, H. A., & Tuukkanen, J. (2007). Effect of modified pectin molecules on the growth of bone cells. *Biomacromolecules*, *8*, 509–515.

Mantovani, M. S., Bellini, M. F., Angeli, J. P. F., Oliveira, R. J., Silva, A. F., & Ribeiro, L. R. (2008). β-Glucans in promoting health: Prevention against mutation and cancer. *Mutation Research*, *658*, 154–161.

Mazumder, S., Morvan, C., Thakur, S., & Ray, B. (2004). Cell wall polysaccharides from Chalkumra (*Benincasa hispida*) fruit. Part I. Isolation and characterization of pectins. *Journal of Agricultural and Food Chemistry*, *52*, 3556–3562.

Mucke, L. (2009). Alzheimer's disease. *Nature*, *461*, 495–497.

Newman, D. J., & Cragg, G. M. (2007). Natural products as sources of new drugs over the last 25 years. *Journal of Natural Products*, *70*, 461–477.

Newman, D. J., & Cragg, G. M. (2012). Natural products as sources of new drugs over the 30 years from 1981 to 2010. *Journal of Natural Products*, *75*, 311–335.

Nie, S.-P., Wang, C., Cui, S. W., Wang, Q., Xie, M.-Y., & Phillips, G. O. (2013). The core carbohydrate structure of Acacia seyal var. seyal (Gum arabic). *Food Hydrocolloids*, *32*, 221–227.

Olson, R. E., & Christ, D. D. (1996). Plasma protein binding of drugs. *Annual Reports in Medicinal Chemistry*, *31*, 327–336.

Ozaki, S., Oki, N., Suzuki, S., & Kitamura, S. (2010). Structural characterization and hypoglycemic effects of arabinogalactan-protein from the *Tuberous cortex* of the White-skinned sweet potato (*Ipomoea batatas* L.). *Journal of Agricultural and Food Chemistry*, *58*, 11593–11599.

Park, J. M., Muhoberac, B. B., Dubin, P. L., & Xia, J. (1992). Effects of protein charge heterogeneity in protein polyelectrolyte complexation. *Macromolecules*, *25*, 290–295.

Peters, T., Jr. (1985). Serum albumin. *Advances in Protein Chemistry*, *37*, 161–245.

Puri, A., Saxena, R., Saxena, R. P., Saxena, K. C., Srivastava, V., & Tandon, J. S. (1993). Immunostimulant agents from *Andrographis paniculata*. *Journal of Natural Products*, *56*, 995–999.

Reddy, M. V. B., Kishore, P. H., Rao, C. V., Gunasekar, D., Caux, C., & Bodo, B. (2003). New 20-oxygenated flavonoids from *Andrographis affinis*. *Journal of Natural Products*, *66*, 295–297.

Sandborn, W. J., Targan, S. R., Byers, V. S., Rutty, D. A., Mu, H., Zhang, X., et al. (2013). *Andrographis paniculata* extract (HMPL-004) for active ulcerative colitis. *The American Journal of Gastroenterology*, *108*, 90–98.

Shu, Y., Liu, M., Chen, S., Chen, X., & Wang, J. (2011). New insight into molecular interactions of imidazolium ionic liquids with bovine serum albumin. *The Journal of Physical Chemistry B*, *115*, 12306–12314.

Sims, I. M., & Bacic, A. (1995). Extracellular polysaccharides from suspension cultures of *Nicotiana plumbaginifolia*. *Phytochemistry*, *38*, 1397–1405.

Sims, I. M., & Furneaux, R. H. (2003). Structure of the exudate gum from *Meryta sinclairii*. *Carbohydrate Polymer*, *52*, 423–431.

Sweet, D. P., Shapiro, R. H., & Albersheim, P. (1975). Quantitative analysis by various g.l.c. response-factor theories for partially methylated and partially ethylated alditol acetates. *Carbohydrate Research*, *40*, 217–225.

Thakur, M., Weng, A., Fuchs, H., Sharma, V., Bhargava, C. S., & Chauhan, N. S. (2012). Rasayana properties of ayurvedic herbs: Are polysaccharides a major contributor. *Carbohydrate Polymer*, *87*, 3–15.

Xu, C., Chou, G., Wang, C., & Wang, Z. (2012). Rare noriridoids from the roots of *Andrographis paniculata*. *Phytochemistry*, *77*, 275–279.

Xu, Y., Dong, Q., Qiu, H., Cong, R., & Ding, K. (2010). Structural characterization of an arabinogalactan from *Platycodon grandiflorum* roots and antiangiogenic activity of its sulfated derivative. *Biomacromolecules*, *11*, 2558–2566.

York, W. S., Darvill, A. G., O'Neil, M., Stevenson, T. T., & Albersheim, P. (1985). Isolation and characterization of plant cell walls and cell wall components. *Methods in Enzymology*, *118*, 3–40.

Zhao, X. C., Liu, R. T., Chi, Z. X., Teng, Y., & Qin, P. F. (2010). New insights into the behavior of bovine serum albumin adsorbed onto carbon nanotubes: Comprehensive spectroscopic studies. *The Journal of Physical Chemistry B*, *114*, 5625–5631.